



Technical paper

Domain reduction method: formulation, possibilities, and examples for analyzing seismic soil-structure interactionBorko Miladinović^{*1)}¹⁾ *University of Montenegro, Faculty of Civil Engineering, Džordža Vašingtona Street, 81000 Podgorica, Montenegro**Article history*

Received: 13 May 2023

Received in revised form:

12 July 2023

Accepted: 27 August 2023

Available online: 30 September 2023

*Keywords*construction and building materials,
earthquake,
soil-structure interaction,
Domain Reduction Method**ABSTRACT**

The Domain Reduction Method (DRM) enables the analysis of seismic soil-structure interaction in a different way compared to other seismic methods. Additionally, it allows certain very important aspects of the mentioned interaction, which are ignored in the usual seismic methods for justified reasons, to be addressed. All this, as well as the fact that this method is still unknown to the professional public and has not been implemented in modern seismic standards, motivated the writing of a paper in which the formulation of the DRM was first presented in detail. Then, the possibilities and approaches to its application in engineering practice were analyzed. In the end, simple dynamic analyses of the seismic interaction of the foundation soil and the pile-supported structure are performed using the DRM, a very specific and insufficiently researched type of seismic soil-structure interaction. Among other things, the results of the performed linear-elastic analyses point to the eventual possibility that the Lateral force seismic method, which is recommended by the Eurocode 8 standard for regular structures and which is most often used in engineering practice, underestimates the level of the lateral seismic load of pile-supported structures. A correct assessment of the seismic load is a fundamental requirement for ensuring a sufficient level of seismic resistance in structures.

1 Introduction

This paper presents a novel method for analyzing seismic soil-structure interaction, which is still relatively unknown among professionals and the scientific community. Known as the Domain Reduction Method (DRM), it was formulated approximately 20 years ago by Bielak et al. [1] and brought about a significant innovation from conventional seismic methods, making it a true "small" revolution. This is also the reason why the DRM encountered disputes at the beginning. Over time, these disputes become less intense, and this seismic method is more and more accepted by the professional and scientific public. However, regardless of the numerous advantages of the DRM, it is still much less frequently used compared to other seismic methods. The formulation of the DRM presented in this paper is taken from: Bielak et al. [1], Youshimura et al. [2], Kantoe et al. [3], and Jeremic et al. [4]. After the formulation of the DRM, the possibilities and ways of its application in engineering practice will be analyzed. Finally, some simple examples of the application of the DRM are presented.

1.1 Development and application of the DRM

The DRM enables the formation and processing of complex seismological (geophysical) 3D numerical models

that contain the earthquake source (i.e., fault), wave propagation paths, and local geological and topographical structures [2]. Also, this method enables the formation complex 3D numerical soil-structure models and simulating real seismic excitation in these models, although they don't contain earthquake source and wave propagation paths. For this reason, the DRM is very suitable for the analysis of dynamic (seismic) soil-structure interactions. Essentially, the dimensions of the foundation soil domain during the formation of numerical soil-structure models are reduced by changing the governing variables [3].

The basic idea of the DRM, which implies the reduction of the dimensions of the soil domain by replacing the governing variables with the assumption that the ground motion during an earthquake in the absence of the structure (free-field ground motion) is known, was presented for the first time by Herrera & Bielak [5]. Also, they proposed an analytical solution on how to determine the displacements of the structure and the soil around the structure during an earthquake based on the known free-field ground motion during an earthquake. The procedures for solving this problem using the finite element method were defined by Bielak and Christiano [6]. In both procedures, seismic excitation is replaced by effective seismic forces applied along the contours of the reduced soil domain. However, the problem with these procedures is that they required the

^{*} Corresponding author:E-mail address: borkom@ucg.ac.me

determination of unknown effective seismic forces in order to define free-field ground motion. Bielak et al. [1] suggested the two-step procedure as a solution to this problem. In this way, the final formulation of the DRM, which is presented in this paper, was obtained. Kontoe et al. [3] suggested the formulation of the DRM for dynamic coupled consolidation analysis.

Regardless of its quality and reliability, the DRM is rarely used in engineering practice. There are two main reasons for this. Firstly, the DRM is still not "recognized" by seismic standards. The exception is the ASCE/SEI 4-16 [7] standard, which proposes the application of this method in seismic resistance analyses of nuclear facilities. There are several works on this topic in the professional and scientific literature [8-12]. Secondly, the DRM has not yet been implemented in the software most commonly used in engineering practice for the design of structures.

1.2 A brief overview of methods for seismic soil-structure interaction analysis

In the middle of the last century, it became clear to engineers that in order to assess the real seismic response of a structure, it is necessary to analyze the interaction of that structure and the foundation soil during an earthquake. Since then, several methods have been developed for the analysis of seismic soil-structure interaction (hereinafter seismic SSI methods). Their development coincides with the development of software that enables more complicated and demanding analysis of structures using numerical methods.

The seismic SSI methods can be divided in several ways. Depending on the method of soil modelling, seismic SSI methods with discrete and continuum soil modelling are distinguished. In discrete soil modelling, the soil is replaced by a series of springs, or springs and dashpots (rheological elements). In continuum soil modelling, appropriate finite and/or boundary elements are most often used. Depending on the material characteristics of the elements used in soil or structural element modelling, the seismic SSI methods can be linear or nonlinear. Usually, only material nonlinearity is considered. However, in situations with intensive yielding of structural elements and/or with intensive yielding of soil (liquefaction), material and geometric nonlinearity must be taken into account. Some seismic SSI methods involve solving the equation of motion of the soil-structure system in the frequency domain. Other seismic SSI methods involve solving the equation of motion of the soil-structure system in the time domain. Methods that use the frequency domain are simpler, but they are not suitable for analyzing the nonlinear behavior of the soil-structure system during an earthquake. A special group consists of the so-called hybrid methods that use both domains.

All seismic SSI methods are based on two main approaches. These are direct and substructure approaches. For this reason, we can talk about direct and substructure seismic SSI methods. In the direct seismic SSI method ("one-step" method), the equation of motion of the complete soil-structure system is solved at once (in one step), usually with free-field ground motion as the input load of the system and usually in the time domain. In the substructure seismic SSI method ("two-step" method), the equation of motion of the system, which contains only the so-called substructure (soil and structural foundation) with free-field ground motion as an input load, is solved first (kinematic interaction) in order to obtain displacements (accelerations, velocities) of the

structural foundation during an earthquake. In this case, some methods take into account the real stiffness of the structural foundation. Other methods assume that the structural foundation is rigid. In the second step, the equation of motion of the system, which contains the superstructure, springs, and dashpots (or more complex nonlinear elements to represent stiffness and damping of the substructure), is solved (inertial interaction) with the previously determined seismic response of the structural foundation as the input load. Frequency-dependent stiffness and damping of the substructure represent so-called dynamic impedances of the foundation. Finally, the results of kinematic and inertial interactions are superimposed.

All previously mentioned seismic SSI methods are also applicable in analyzes of the interaction between the soil and the pile-supported structure during an earthquake (seismic SPS interaction). Piles are usually modelled using a beam of finite elements. The contact between the surrounding soil and the piles is simulated using discrete rheological elements (springs, springs, and dashpots, etc.) or interface finite elements. In the substructure seismic SSI method, the first step involves solving the equation of motion of the system, which consists of soil, piles, and pile caps. In the second step, it is necessary to define the dynamic impedances of the pile foundation.

2 Formulation of the domain reduction method

Fig. 1a shows a very simplified engineering, and seismo-geological model of the region of interest. A simple fault that represents a potential source of an earthquake is also modeled. Models of this type are usually kilometers in size, and seismologists use them to analyze the seismic hazards of the region of interest. The seismic excitation of the region of interest, considering the assumed fault type and characteristics, is defined by analyzing the generated model, typically in the form of displacement, velocity, and acceleration fields. So, in this way, the seismic excitation in the zone of any object (structure) within the treated region is defined. However, it is impossible to analyze the soil-structure interaction for any object during an earthquake on a model of these dimensions. In order to analyze this interaction, the question arises as to how only a smaller zone of soil around the object of interest can be separated from the formed and processed seismo-geological model, but in such a way that the previously defined seismic excitation remains "trapped" in it (see Fig. 1b). The solution is given by Bielak et al. [1], who formulate the DRM.

Γ marks the boundary between the outside soil subdomain Ω^+ and the inside soil subdomain Ω . This boundary is taken into account in the seismic soil-structure interaction analysis for the object of interest. The dimensions of the inside domain are usually 3-4 times larger than the dimensions of the object. Nodal displacements of the outside subdomain Ω^+ , inside subdomain Ω , and boundary between them Γ are denoted by u_e , u_i and u_b respectively. So, the subscripts i , e and b refer to the part of the analysed soil domain to which some quantity refers. For the analysed soil domain, the equation of motion in the case of forced undamped oscillations can be expressed in matrix form as:

$$\mathbf{M} \cdot \ddot{\mathbf{u}} + \mathbf{K} \cdot \mathbf{u} = \mathbf{P}_e \quad (1)$$

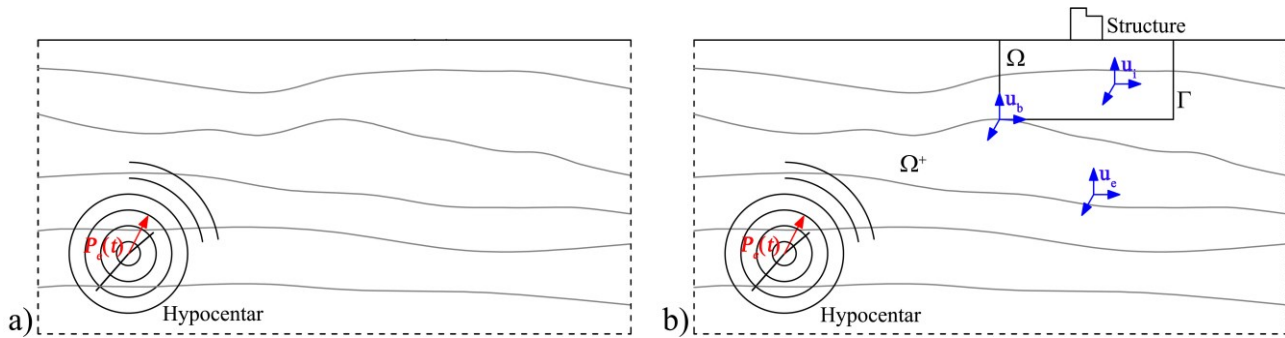


Figure 1. a) The seismo-geological model of the region of interest with a potential source of earthquake
 b) Division of the seismo-geological model domain into two subdomains. (Adapted from [1])

or can be expressed in partitioned form for both soil subdomains as:

$$\begin{bmatrix} \mathbf{M}_{ii}^{\Omega} & \mathbf{M}_{ib}^{\Omega} & 0 \\ \mathbf{M}_{bi}^{\Omega} & \mathbf{M}_{bb}^{\Omega} + \mathbf{M}_{bb}^{\Omega^+} & \mathbf{M}_{be}^{\Omega^+} \\ 0 & \mathbf{M}_{eb}^{\Omega^+} & \mathbf{M}_{ee}^{\Omega^+} \end{bmatrix} \cdot \begin{Bmatrix} \ddot{\mathbf{u}}_i \\ \ddot{\mathbf{u}}_b \\ \ddot{\mathbf{u}}_e \end{Bmatrix} + \begin{bmatrix} \mathbf{K}_{ii}^{\Omega} & \mathbf{K}_{ib}^{\Omega} & 0 \\ \mathbf{K}_{bi}^{\Omega} & \mathbf{K}_{bb}^{\Omega} + \mathbf{K}_{bb}^{\Omega^+} & \mathbf{K}_{be}^{\Omega^+} \\ 0 & \mathbf{K}_{eb}^{\Omega^+} & \mathbf{K}_{ee}^{\Omega^+} \end{bmatrix} \cdot \begin{Bmatrix} \mathbf{u}_i \\ \mathbf{u}_b \\ \mathbf{u}_e \end{Bmatrix} = \begin{Bmatrix} 0 \\ 0 \\ \mathbf{P}_e \end{Bmatrix} \quad (2)$$

On the left side of Eq. (2), the matrices \mathbf{M} and \mathbf{K} denote the mass and stiffness submatrices, the vectors $\ddot{\mathbf{u}}$ and \mathbf{u} denote the nodal accelerations and displacements subvectors. On the right side of Eq. (2), vector \mathbf{P}_e denotes the subvector of unknown seismic nodal forces. The outside soil subdomain Ω^+ and the inside soil subdomain Ω with the object of interest can be separated from each other. Therefore, the above equation can be simply divided into two equations as follows:

But it is very important to remember that the inside and outside soil subdomains and their equations of motion are separated based on the assumption that nodal displacements u_b and nodal forces P_b are compatible along the boundary between the two soil subdomains (see Fig. 2a).

$$\begin{bmatrix} \mathbf{M}_{ii}^{\Omega} & \mathbf{M}_{ib}^{\Omega} \\ \mathbf{M}_{bi}^{\Omega} & \mathbf{M}_{bb}^{\Omega} \end{bmatrix} \cdot \begin{Bmatrix} \ddot{\mathbf{u}}_i \\ \ddot{\mathbf{u}}_b \end{Bmatrix} + \begin{bmatrix} \mathbf{K}_{ii}^{\Omega} & \mathbf{K}_{ib}^{\Omega} \\ \mathbf{K}_{bi}^{\Omega} & \mathbf{K}_{bb}^{\Omega} \end{bmatrix} \cdot \begin{Bmatrix} \mathbf{u}_i \\ \mathbf{u}_b \end{Bmatrix} = \begin{Bmatrix} 0 \\ \mathbf{P}_b \end{Bmatrix} \quad \text{for inside soil subdomain } \Omega \quad (3)$$

$$\begin{bmatrix} \mathbf{M}_{bb}^{\Omega^+} & \mathbf{M}_{be}^{\Omega^+} \\ \mathbf{M}_{eb}^{\Omega^+} & \mathbf{M}_{ee}^{\Omega^+} \end{bmatrix} \cdot \begin{Bmatrix} \ddot{\mathbf{u}}_b \\ \ddot{\mathbf{u}}_e \end{Bmatrix} + \begin{bmatrix} \mathbf{K}_{bb}^{\Omega^+} & \mathbf{K}_{be}^{\Omega^+} \\ \mathbf{K}_{eb}^{\Omega^+} & \mathbf{K}_{ee}^{\Omega^+} \end{bmatrix} \cdot \begin{Bmatrix} \mathbf{u}_b \\ \mathbf{u}_e \end{Bmatrix} = \begin{Bmatrix} -\mathbf{P}_b \\ \mathbf{P}_e \end{Bmatrix} \quad \text{for outside soil subdomain } \Omega^+ \quad (4)$$

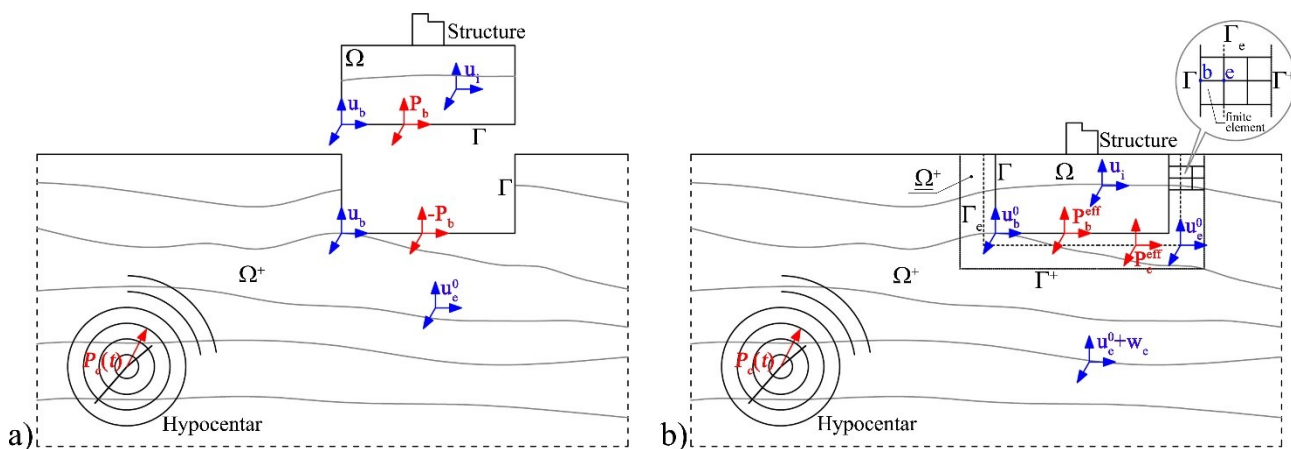


Figure 2. a) Separated inside and outside soil subdomain of the analysed seismo-geological model
 b) Dimension reduction of the outside soil subdomain, DRM and Damping layer

Eq. (4) is used for the elimination of the unknown values of the seismic nodal forces P_e from Eq. (2). Since Eq. (4) is valid for the separated outside soil subdomain Ω^+ , so there is no influence of the inside subdomain and the object, the values of outside nodal displacements u_e and accelerations \ddot{u}_e actually correspond to the values of outside nodal displacements and accelerations calculated for the free-field soil model (free-field outside nodal displacements and accelerations) u_e^0 and \ddot{u}_e^0 . In that case, Eq. (4) can be written as:

$$\begin{bmatrix} \mathbf{M}_{bb}^{\Omega^+} & \mathbf{M}_{be}^{\Omega^+} \\ \mathbf{M}_{eb}^{\Omega^+} & \mathbf{M}_{ee}^{\Omega^+} \end{bmatrix} \cdot \begin{Bmatrix} \ddot{\mathbf{u}}_b^0 \\ \ddot{\mathbf{u}}_e^0 \end{Bmatrix} + \begin{bmatrix} \mathbf{K}_{bb}^{\Omega^+} & \mathbf{K}_{be}^{\Omega^+} \\ \mathbf{K}_{eb}^{\Omega^+} & \mathbf{K}_{ee}^{\Omega^+} \end{bmatrix} \cdot \begin{Bmatrix} \mathbf{u}_b^0 \\ \mathbf{u}_e^0 \end{Bmatrix} = \begin{Bmatrix} -\mathbf{P}_b^0 \\ \mathbf{P}_e \end{Bmatrix} \quad (5)$$

The free-field outside nodal displacements and accelerations are already known because of how the free-field seismo-geological model shown in Fig. 1a was made and how it was used. Therefore, the above equation can be used to calculate the unknown seismic nodal forces P_e . These forces are equal to:

$$\mathbf{P}_e = \mathbf{M}_{eb}^{\Omega^+} \cdot \ddot{\mathbf{u}}_b^0 + \mathbf{M}_{ee}^{\Omega^+} \cdot \ddot{\mathbf{u}}_e^0 + \mathbf{K}_{eb}^{\Omega^+} \cdot \mathbf{u}_b^0 + \mathbf{K}_{ee}^{\Omega^+} \cdot \mathbf{u}_e^0 \quad (6)$$

According to the main assumption and transformation of the DRM, the displacement of any node in the outside soil subdomain Ω^+ can be expressed in the form of the following sum of displacements:

$$\mathbf{u}_e = \mathbf{u}_e^0 + \mathbf{w}_e \quad (7)$$

where \mathbf{w}_e represent a vector of "residual" displacement field, i.e., a vector of relative displacement field with respect to the reference vector of free field displacement \mathbf{u}_e^0 . Actually, in the above equation, in terms of the vector \mathbf{w}_e represent the changes in the free-field outside nodal displacements caused by the oscillation of the object (structure) during an earthquake. After substituting Eq. (7) into Eq. (2), the equation of motion for the analyzed soil domain can be written as:

$$\begin{bmatrix} \mathbf{M}_{ii}^{\Omega} & \mathbf{M}_{ib}^{\Omega} & 0 \\ \mathbf{M}_{bi}^{\Omega} & \mathbf{M}_{bb}^{\Omega} + \mathbf{M}_{bb}^{\Omega^+} & \mathbf{M}_{be}^{\Omega^+} \\ 0 & \mathbf{M}_{eb}^{\Omega^+} & \mathbf{M}_{ee}^{\Omega^+} \end{bmatrix} \cdot \begin{Bmatrix} \ddot{\mathbf{u}}_i \\ \ddot{\mathbf{u}}_b \\ \ddot{\mathbf{u}}_e^0 + \ddot{\mathbf{w}}_e \end{Bmatrix} + \begin{bmatrix} \mathbf{K}_{ii}^{\Omega} & \mathbf{K}_{ib}^{\Omega} & 0 \\ \mathbf{K}_{bi}^{\Omega} & \mathbf{K}_{bb}^{\Omega} + \mathbf{K}_{bb}^{\Omega^+} & \mathbf{K}_{be}^{\Omega^+} \\ 0 & \mathbf{K}_{eb}^{\Omega^+} & \mathbf{K}_{ee}^{\Omega^+} \end{bmatrix} \cdot \begin{Bmatrix} \mathbf{u}_i \\ \mathbf{u}_b \\ \mathbf{u}_e^0 + \mathbf{w}_e \end{Bmatrix} = \begin{Bmatrix} 0 \\ 0 \\ \mathbf{P}_e \end{Bmatrix} \quad (8)$$

As stated previously, the values of free-field outside nodal displacements and accelerations (u_e^0 and \ddot{u}_e^0) are known. Therefore, they can be moved to the right side of the above equation. Lastly, substituting Eq. (6) into Eq. (8), the equation of motion for the analyzed soil domain in the case of forced undamped oscillations can be written as:

$$\begin{bmatrix} \mathbf{M}_{ii}^{\Omega} & \mathbf{M}_{ib}^{\Omega} & 0 \\ \mathbf{M}_{bi}^{\Omega} & \mathbf{M}_{bb}^{\Omega} + \mathbf{M}_{bb}^{\Omega^+} & \mathbf{M}_{be}^{\Omega^+} \\ 0 & \mathbf{M}_{eb}^{\Omega^+} & \mathbf{M}_{ee}^{\Omega^+} \end{bmatrix} \cdot \begin{Bmatrix} \ddot{\mathbf{u}}_i \\ \ddot{\mathbf{u}}_b \\ \ddot{\mathbf{w}}_e \end{Bmatrix} + \begin{bmatrix} \mathbf{K}_{ii}^{\Omega} & \mathbf{K}_{ib}^{\Omega} & 0 \\ \mathbf{K}_{bi}^{\Omega} & \mathbf{K}_{bb}^{\Omega} + \mathbf{K}_{bb}^{\Omega^+} & \mathbf{K}_{be}^{\Omega^+} \\ 0 & \mathbf{K}_{eb}^{\Omega^+} & \mathbf{K}_{ee}^{\Omega^+} \end{bmatrix} \cdot \begin{Bmatrix} \mathbf{u}_i \\ \mathbf{u}_b \\ \mathbf{w}_e \end{Bmatrix} = \begin{Bmatrix} 0 \\ -\mathbf{M}_{be}^{\Omega^+} \cdot \ddot{\mathbf{u}}_e^0 - \mathbf{K}_{be}^{\Omega^+} \cdot \mathbf{u}_e^0 \\ \mathbf{M}_{eb}^{\Omega^+} \cdot \ddot{\mathbf{u}}_b^0 + \mathbf{K}_{eb}^{\Omega^+} \cdot \mathbf{u}_b^0 \end{Bmatrix} \quad (9)$$

It is already known what the terms of the above equation represent. All unknowns are on the left side of the equation. The vector on the right side of the equation represents the seismic effective nodal force vector. This vector can be written as:

$$\mathbf{P}^{eff} = \begin{Bmatrix} \mathbf{P}_i^{eff} \\ \mathbf{P}_b^{eff} \\ \mathbf{P}_e^{eff} \end{Bmatrix} = \begin{Bmatrix} 0 \\ -\mathbf{M}_{be}^{\Omega^+} \cdot \ddot{\mathbf{u}}_e^0 - \mathbf{K}_{be}^{\Omega^+} \cdot \mathbf{u}_e^0 \\ \mathbf{M}_{eb}^{\Omega^+} \cdot \ddot{\mathbf{u}}_b^0 + \mathbf{K}_{eb}^{\Omega^+} \cdot \mathbf{u}_b^0 \end{Bmatrix} \quad (10)$$

The seismo-geological model (see Fig. 1a) shows that the seismic effective nodal forces P_e^{eff} always replace the seismic nodal forces P_e that are made by the fault crack. Consequently, using seismic effective nodal forces P_e^{eff} , all real seismic waves (P, SV, SH, Rayleigh and Love waves) can be adequately modelled. According to Eq. (10), in order to define the forces P_e^{eff} , the values of free-field nodal accelerations and displacements (\ddot{u}_e^0 and u_e^0) are necessary. However, it is very interesting and significant to state that in Eq. (10) these accelerations and displacements are multiplied only with the mass and stiffness matrices of those finite elements of the outside soil subdomain Ω^+ that are located along the boundary Γ , i.e., between the boundaries Γ and its adjacent boundary Γ_e (see Fig. 2b). The boundary Γ_e represents an outside contour (surface) of the fictitious soil layer, which will be discussed a little later and is particularly important in the DRM. Therefore, the seismic effective nodal forces P_e^{eff} act only on the nodes of the finite elements of the outside soil subdomain located between the boundaries Γ and Γ_e . For this reason, in order to determine the intensity of forces P_e^{eff} , it is necessary to know the values of accelerations \ddot{u}_0 and displacements u_0 only for those nodes. In order to simplify the calculation, i.e., reduce the number of unknown effective nodal forces P_e^{eff} that must be determined, it can be assumed that the boundaries Γ and Γ_e are close enough to each other, so there is only one layer of finite elements between them. In this situation, the seismic effective forces P_e^{eff} act only on the nodes of that one layer of finite elements. This layer of finite elements is called the DRM layer. This localization of forces P_e^{eff} is a direct consequence of the outside subdomain nodal displacement transformation, i.e., a direct consequence of Eq. (7).

In addition to the previously described method of defining the seismic load, the DRM's expression of the equation of motion (Eq. (9)). As can be seen, the unknowns in this equation are only displacements of the nodes on the boundaries Γ and Γ_e (see Fig. 2b). For the outside soil subdomain Ω^+ i.e., part of the soil beyond the boundary Γ_e , the "residual" displacement field w_e is obtained by solving Eq. (9). The "residual" displacement field w_e is relative displacement field with respect to the primary displacement field u^0 (free-field displacements). In the soil-structure interaction analyses, attention is focused on the structure and the foundation soil. For this reason, this "residual" displacement field has no practical significance. This fact, as well as the previously described way of defining the seismic load in the DRM, allows a drastic reduction of the complete outside soil subdomain to a smaller soil subdomain $\underline{\Omega}^+$ around the DRM layer, i.e., the subdomain between the boundaries Γ_e and Γ^+ (see Fig. 2b). Due to the possibility of reducing the dimensions of the soil domain, this seismic method is called the Domain Reduction Method (DRM). A sufficiently high damping level should be adopted for the material of the reduced outside soil subdomain $\underline{\Omega}^+$, in order to prevent the occurrence of spurious seismic waves. These waves can be generated by waves from the inside soil subdomain passing through the outside soil subdomain, hitting the model boundary, and being reflected back to the inside soil subdomain and structure. The reduced outside soil subdomain $\underline{\Omega}^+$ with pronounced material damping is called the Damping layer and is modeled with two or more layers of finite elements.

Two very significant facts of the DRM that refer to the reduced outside soil subdomain $\underline{\Omega}^+$ i.e., the Damping layer, should be mentioned. First, according to the main assumption, i.e., the transformation of the DRM (Eq. (7)), outside subdomain nodal displacements are obtained by applying the principle of superposition. In most cases, the main reason for disputing the DRM by the professional and scientific public was related to this transformation. It is generally known that the principle of superposition can be applied only in the case of elastic materials, i.e., only in the case of linear-elastic analyses. However, the disputed principle of superposition (Eq. (7)) is only valid for the outside soil subdomain $\underline{\Omega}^+$. Therefore, it does not apply to the structure, and it does not apply to the foundation soil, i.e., inside soil subdomain Ω . It is only valid for the soil that is located at a sufficiently large distance from the structure, i.e., for the outside soil subdomain $\underline{\Omega}^+$. This soil subdomain is not of interest in the soil-structure interaction analyses. So, engineers, when using the DRM, should not be concerned about the adopted assumption related to the linear-elastic behavior of the outside soil subdomain material.

The previous statement, related to the superposition of outside subdomain nodal displacements, can also be accepted for the high level of damping that is adopted for the outside soil subdomain $\underline{\Omega}^+$ i.e., for the Damping layer. This is the second important fact that should be mentioned. In this way, a very significant problem in the dynamic soil-structure interaction analysis is easily overcome. It is a problem of boundary conditions along the artificial boundaries of the modeled soil domain (model boundaries). In the usual methods of analyzing the seismic soil-structure interaction, viscous dampers, i.e., dashpots, are placed along these boundaries. Their task is to absorb seismic waves that hit the model boundaries. However, these elements only absorb waves that hit the model boundaries at the right angle. So, if the wave hits the model boundary at some oblique angle, the

effectiveness of the dashpots is problematic. The adoption of a high level of damping for the Damping layer in the DRM enables the placement of the simplest supports (pins or rollers) along the model boundaries. Also, it enables seismic excitation to be applied to the soil-structure system in any direction. This opens up new possibilities in seismic soil-structure interaction analyses.

Based on what has been said, it can be said that if the DRM is used, it is necessary to define the material properties of two more fake soil layers in addition to the material properties of the inside soil subdomain Ω (inside soil). It is the DRM and Damping layer. Usually, linear-elastic materials with all the same characteristics except damping are adopted for those soil layers. The material of the Damping layer has a high level of damping, while the DRM layer is without damping. All other material characteristics of the DRM and Damping layer are identical, and their values are adopted based on the values of the inside soil material characteristics.

3 Use of the DRM in engineering practice

Regardless of its quality and reliability, the previously described DRM is rarely used in engineering practice. Unfortunately, the DRM has not yet been implemented in the software most commonly used in engineering practice for the design of structures. Therefore, the use of the DRM is mainly related to scientific research in the field of seismic soil-structure interaction.

According to Eq. (10), in order to use DRM to analyze the interaction of foundation soil and structure at some location during an earthquake, it is necessary to define the seismic excitation for that location. Defining the seismic excitation implies the determination of the values of free-field displacements u^0 and accelerations \ddot{u}^0 for all nodes of the DRM layer, which are necessary for calculating the intensity of effective seismic forces. Generally, these values are obtained by processing the seismo-geological model of the location of interest, i.e., the wider area to which the location belongs. However, models of this type are very rare. So far, such a seismo-geological model for any part of Montenegro has not been formed. Therefore, some alternative solutions are usually applied. These solutions imply the use of appropriate recordings of previous earthquakes. If there are recordings of free-field ground motions during previous earthquakes for the location (area) where the analyzed object is located, this can be a very favorable circumstance for engineers when implementing the DRM. In these situations, existing unscaled or scaled recordings can be used as input data for the DRM, i.e., as so-called input accelerograms for the DRM. However, if these recordings do not exist for a location of interest, then appropriate scaled or unscaled recordings of previous earthquakes downloaded from one of the many Internet Ground Motion Databases (GMDB) are used as input accelerograms for the DRM. Examples can be singled out: the European Strong-Motion Database (ESD), the Engineering Strong-Motion Database (ESM), and the PEER Ground Motion Database (Pacific Earthquake Engineering Research Center). However obtained, the input accelerograms and their corresponding displacement recordings are used to determine the values of free-field displacements u^0 and accelerations \ddot{u}^0 for all nodes of the DRM layer. According to Eq. (10), if these accelerations and displacements are known, the intensities of the effective seismic forces can be calculated, which provides the conditions for the application of the DRM.

Usually, corrected acceleration recordings (and often also velocity and displacement) can be downloaded from the GMBD for a specific earthquake and location (seismograph station) in two horizontal directions that are perpendicular to each other (East-West and North-South) and in the vertical direction. Thus, there are three components of acceleration and three components of displacement. So far, earthquakes with two or only one component of displacement (acceleration) have not been registered. Engineers interpret the downloaded recordings by considering that every "point" on or in the soil (hereinafter soil point), i.e., on or in the structure (depending on where the seismograph is placed), was exposed to displacements in the direction of all three axes during an earthquake. However, this interpretation is only partially correct because any point at and near the soil surface (in shallower layers) is also exposed to rotations around all three axes during an earthquake [12-14]. These rotations actually mean different displacements of two adjacent points, i.e., points at a small distance from each other. So, instead of three, there are actually six displacement components. On concrete numerical models, Jeremić et al. [4] showed a significantly different seismic response of the soil in the case when only the previously described componential displacements are taken into account and in the case when both componential displacements and componential rotations are taken into account.

In the DRM, the input accelerograms and their corresponding displacement recordings can be used in different ways to determine the values of accelerations \ddot{u}^0 and displacements u^0 of all nodes of the DRM layer. These accelerations and displacements are needed to calculate the effective seismic forces. The simplest way, but also the one that least corresponds to the real situation, implies the complete neglect of the previously mentioned seismic rotations of the soil points (soil particles). Input accelerograms and their corresponding displacement recordings are "joined" to the displacement directions of the soil points. After that, the position of the reference point (coordinate z_R) is defined, which is assumed to be the place of registration of the input accelerograms. In the next step, known dynamic methods, which for the soil profile at a given location perform one-dimensional (vertical) propagation of input accelerograms through the soil, are applied. Usually, the linear or possibly equivalent linear method is used. If it is chosen that the reference point is located on the soil surface ($z_R=0$), which is most often the case, then the 1D deconvolution of input accelerograms through the soil profile is actually performed. If it is chosen that the reference point is located at a certain depth ($z_R<0$) e.g., the level of the bedrock, then the 1D convolution of input accelerograms through the soil profile is actually performed. Depending on the type of analysis performed, regardless of the position of the reference point, with this 1D propagation of the input accelerogram through the soil profile, for each point of this profil, the values of one, two, or all three components of the acceleration \ddot{u}^0 or displacement u^0 during an earthquake are determined. Finally, the calculated accelerations and displacements are "joined" to the corresponding nodes of the DRM layer. Thus, according to Eq. (10), the conditions for calculating the intensity of effective seismic forces and using the DRM are obtained.

If the input accelerograms and their corresponding displacement recordings are used in the previously described manner, one can speak of 1×1C, 2×1C or 3×1C DRM depending on how many components of acceleration \ddot{u}^0 and displacement u^0 are taken into account when

calculating the intensity of effective seismic forces. The main shortcoming of these analyses is the fact that when determining accelerations \ddot{u}^0 and displacements u^0 , as necessary data for calculating effective seismic forces, only body seismic waves are taken into account. In other words, the determination of accelerations \ddot{u}^0 and displacement u^0 is performed under the assumption that the movement of the soil during an earthquake is the result of the vertical propagation of P and S body seismic waves from the hypocenter to the soil surface. For this reason, identical displacements of all soil points with the same coordinate z during an earthquake are obtained. This does not correspond to the real situation, especially for soil points at a shallower depth whose movements are dominantly influenced by surface seismic waves. It is known that the influence of surface waves on the seismic excitation to which the structure is exposed can be very significant and often dominant. Surface seismic waves, i.e., their destructiveness, come to the fore in shallow earthquakes (hypocenter depth up to 70km), while deep earthquakes do not produce this type of seismic wave (hypocenter depth greater than 300km).

If the previously described variant of the DRM is correctly implemented, for any soil point with the coordinate $z=z_R$, the input accelerogram and its corresponding displacement recording "joined" to one of the global axes must be identical to the obtained (output) accelerogram and its corresponding displacement recording for that global axis.

Another way in which input accelerograms and their corresponding displacement recordings can be used to calculate the intensity of effective seismic forces is similar to the previous one. The difference is in the adopted direction of seismic wave propagation. Previously, propagation was vertical. Now, it is inclined, i.e., seismic waves propagate from the source of the earthquake to the soil surface at a certain angle θ in relation to the vertical axis (up to 10°, possibly 15°, rarely more). So, this is the case of the inclined convolution of the input accelerogram through the analyzed soil profile. At the beginning, for the purposes of implementing this convolution, it is necessary to define the coordinates of the soil point that is adopted as the source of the seismic excitation (coordinates x_S, y_S, z_S), which are characterized by the adopted accelerogram and its corresponding displacement recording. This point may be within or outside of the boundaries of the numerical model that is formed to implement the DRM. In the described way, in addition to the effects of body seismic waves, the effects of surface seismic waves, which arise as a result of the interaction of the "inclined" body waves and the soil surface, are also tried to be taken into account. The effects of surface waves primarily imply the relative displacement of adjacent points of shallower soil layers during an earthquake, i.e., the occurrence of the previously mentioned seismic rotations of the soil points.

In general, 3C or 6C DRM can be used if the input accelerograms and their corresponding displacement records are used in the way already described. This depends on how the seismic excitation is defined and the type of numerical model. More precisely, if a 2D numerical model of the soil-structure system and the previously described way of applying input accelerograms and their corresponding displacement recordings are used, each soil point is simultaneously subjected to two componential displacements (in the direction of the horizontal and vertical axes – mean axes) and to a componential rotation around an axis perpendicular to the plane of the numerical model. In this case, it is about 3C DRM. If a 3D numerical model of the soil-

structure system and the previously described way of applying input accelerograms and their corresponding displacement recordings are used, each soil point is simultaneously subjected to three componental displacements (in the direction of two horizontal and vertical axes – mean axes) and to componental rotations around all mean axes. In this case, it is about 6C DRM. As already mentioned, these componental rotations actually represent the relative displacements of adjacent soil points during an earthquake.

In the end, it is important to note that the way of simulating seismic excitation in the DRM enables the emergence of surface seismic waves as a "result" of the interaction of inclined body waves with appropriate characteristics (frequency and angle θ relative to vertical axes) and shallower layers of foundation soil [15]. No evidence was found in the professional and scientific literature that this way of simulating surface seismic waves is applicable to other seismic SSI methods.

4 Numerical example

4.1 Input data

The previously formulated DRM is presented and demonstrated on the simple example of the interaction of a two-dimensional (2D) RC pile-supported frame and layered foundation soil during an earthquake (see Fig. 3). For the analyzed system, which consists of the soil, pile foundation, and structure (frame), the term SPS system is used in the following text. Two linear-elastic dynamic analyses are carried out. The first is a 1×1C DRM with vertical, linear convolution of the input accelerogram from the bedrock level ($z_R=-17\text{m}$) to the soil surface. The second, 3C DRM, has a linear, inclined convolution of the input accelerogram ($\theta=10^\circ$) from the soil point with coordinates $x_S=0$, $y_S=0$ and $z_S=-17\text{m}$ to the soil surface. Fig. 4 shows the input accelerogram used in the dynamic analyses. It was downloaded from the ESM. The horizontal seismic excitation at the level of the base of the RC frame, i.e., at the level of the pile cap beam, was first

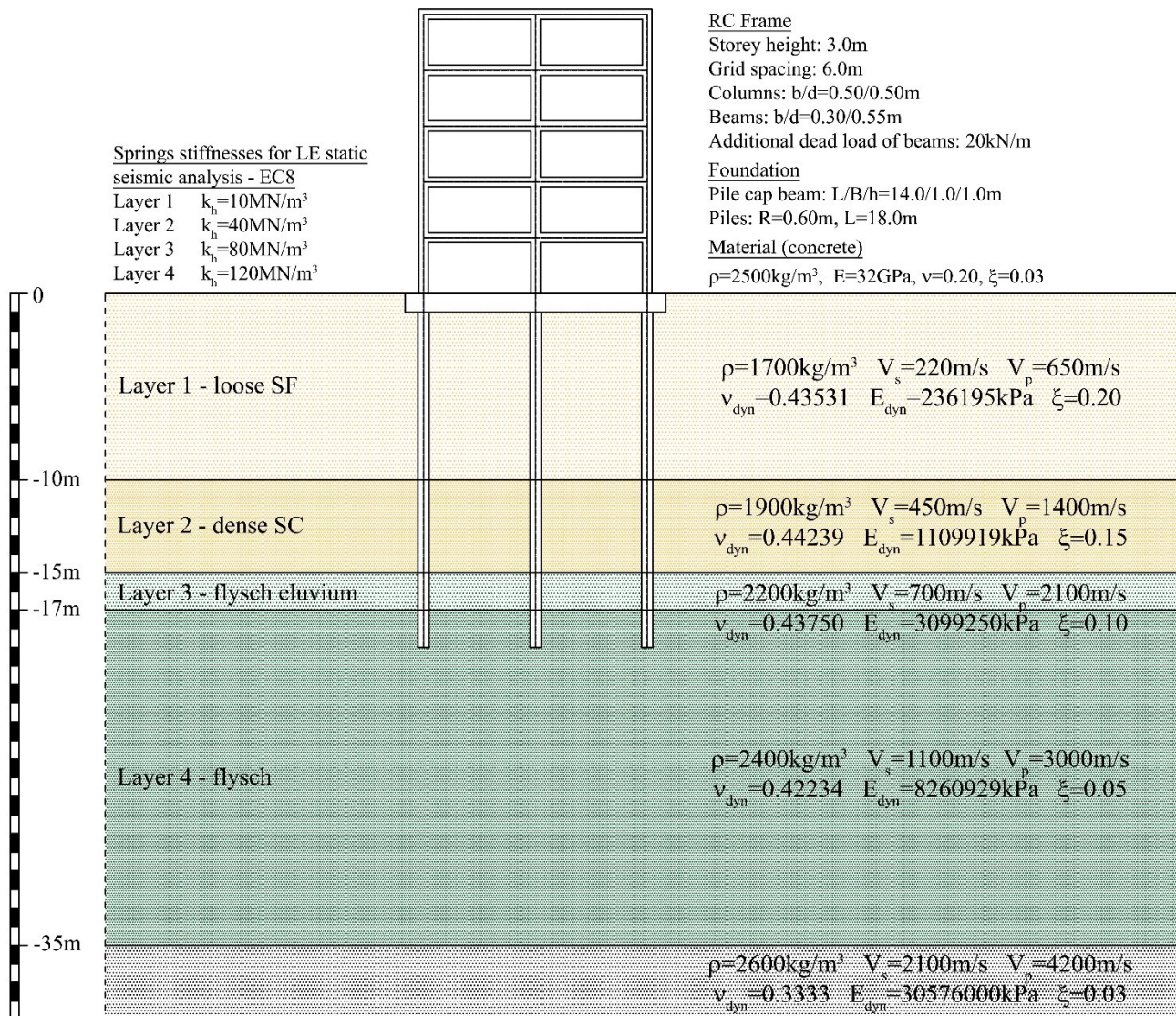


Figure 3. Analyzed SPS system with characteristics of RC frame, foundation and all layers of the foundation soil

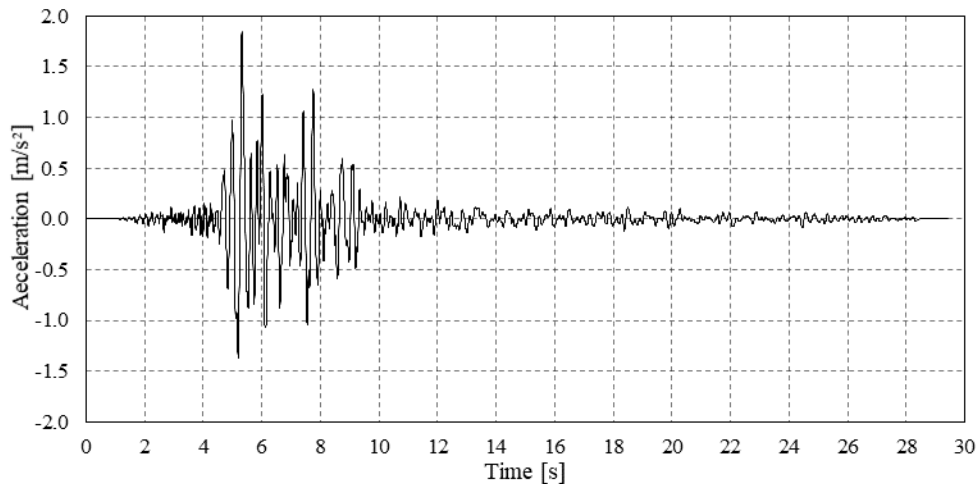


Figure 4. Used accelerogram (26.09.1997., Lower square of St. Francis, comune of Assisi, province of Perugia, region Umbria, Italy, direction East-West, $M_w=6.0$, epicentral distance 21.6km)

determined by using the DRM. After that, it is compared with the given (input) horizontal seismic excitation at the bedrock level. So, the influence of the upper, soft layers of the foundation soil on the seismic response of the RC pile-supported frame is analyzed.

In the end, it was considered highly useful to carry out a linear-elastic, static seismic analysis of the RC pile-supported frame in a manner common (well-known and generally accepted) in engineering practice. The elastic lateral seismic load of the analyzed frame was determined according to the standard Eurocode 8 (Lateral force seismic method) for $a_{g,max}=0.20 \cdot g$ (which corresponds to the input accelerogram), ground type B with $V_{s,30}=456\text{m/s}$, elastic response spectra Type 1 (damping 5%) and importance factor $\gamma=1.0$. The surrounding soil was modeled using linear-elastic springs. Their stiffness k_h has been assessed according to the Vesic solution [16]. The piles, pile caps, beams, and columns were modelled using a beam finite element with appropriate material and geometric characteristics. This analysis was performed using the software Tower 6 (Radimpex). The results of this analysis, with the working title LE static seismic analysis – EC8, will be compared to the results of DRM analyses.

4.2 Model for numerical analysis

In order to perform the previously described dynamic analyses, the numerical model of the analysed SPS system is formed in the software Real-ESSI Simulator (Real-ESSI software), which was developed by Professor Jeremic from UC Davis, California (see Fig. 5). The software is based on the Finite element method. In order to form this model, except for all layers of the foundation soil, it was necessary to define two additional materials. One material for the DRM layer and the other material for the Damping layer. For both of these layers, all material characteristics are adopted as for layer 1 of the foundation soil, except material damping. Rayleigh damping is used in the dynamic analyses. The Rayleigh damping ratio ξ for the DRM layer is equal to zero (no damping), and for the Damping layer is 0.50.

It is well-known that the damping level of seismic waves in the soil increases with the increase in the level of plastic shear deformations in that soil caused by these waves. For this reason, higher values of the Rayleigh damping ratio ξ are adopted for the soil layers 1, 2 and 3. As expected, the

value of this ratio was the highest for the softest layer. A standard value of damping ratio $\xi=0.05$ is adopted for the bedrock (layer 4).

The layered foundation soil is modeled with two identical vertical "screen" of elastic three-dimensional (3D) hexahedral finite elements with eight nodes ($b=l=h=1\text{m}$). Displacements of all nodes in the direction of the Y axis are prevented. The connection of finite elements at the contact between two different layers of foundation soil is "direct" i.e., interface finite elements are not used.

The pile cap beam is modeled with two identical vertical "screen" of elastic 3D hexahedral finite elements with eight nodes ($b/l/h=1.0/1.0/0.25\text{m}$). Displacements of all nodes in the direction of the Y axis are prevented.

All elements of the RC frame as well as the piles are modeled with elastic beam (1D) finite elements with two nodes ($l=1\text{m}$). For these elements, appropriate geometric and material characteristics are defined in accordance with the adopted dimensions of their cross-sections and the characteristics of concrete as a material.

Linear zero-thickness interface finite elements with appropriate normal (axial) stiffness K_N and shear stiffness K_S are used to model the contact between the pile cap beam and soil, i.e., the contact between the piles and surrounding soil. These elements have unlimited axial compressive strength and constant axial stiffness, without tensile strength (stiffness), with constant shear stiffness until the shear strength τ_f is reached. After that, they are without shear stiffness. Of course, their shear strength depends on the level of normal stress, i.e., on the normal stiffness of K_N . Usually, this problem of the mutual dependence of normal and shear stiffness is solved iteratively. The adopted interface's finite elements are without damping. The stiffnesses K_N and K_S are calculated using the following well-known empirical solutions:

$$K_N = \frac{E_{oed,i}}{t_i} = \frac{2 \cdot G_i \cdot (1 - \nu_i)}{(1 - 2 \cdot \nu_i) \cdot t_i} \quad (11a)$$

$$K_S = \frac{G_i}{t_i} = \frac{R \times G}{t_i} \quad (11b)$$

$$\tau_f = \sigma_n \cdot \text{tg}(R \cdot \phi) \quad (11c)$$

where $E_{oed,i}$, ν_i , G_i and t_i denote the oedometric modulus of elasticity, Poisson's coefficient, shear modulus, and fictitious thickness of the interface finite element, respectively. In Eq. (11b) G denotes the shear modulus of the soil. The Poisson's coefficient of the interface finite element is usually 0.45, in order to avoid numerical errors that are common with these elements. The fictitious thickness of the zero-thickness interface finite element is usually from 0.01 to 0.1. In Eq. (11c), R denotes the strength reduction factor, which for the concrete-sand contact is from 0.8 to 1.0, while for the concrete-clay contact it is from 0.7-1.0. In Eq. (11c) ϕ denotes the angle of shear resistance of the soil.

4.3 Results

Figure 6 shows the deformed shape of the analysed SPS system at one moment of seismic excitation for the case 1×1C DRM. In the other images, the results of the performed dynamic analyses are shown in the form of recordings of the horizontal acceleration of the soil or structure during an earthquake. Also, horizontal acceleration elastic response spectra are shown. In those images, the black dashed line (Input) shows the input accelerogram used in the analyses. The black solid line (Output) shows the obtained recording of the horizontal acceleration or obtained horizontal acceleration elastic response spectra at the level of the bedrock for 1×1C DRM i.e. at the point with coordinates $x_R=0$, $y_R=0$ and $z_R=-17\text{m}$ for 3C DRM. The blue solid line (Output_FF) shows the obtained recording of the horizontal acceleration or obtained horizontal acceleration elastic response at the central point on the soil surface of the model without RC frame and piles (free-field model), which was subsequently formed. The red solid line (Output_SPS) shows the obtained recording of the horizontal acceleration or obtained horizontal acceleration elastic response at the base of the structure, i.e., at the center point on the upper edge ($z=0$) of the pile cap beam.

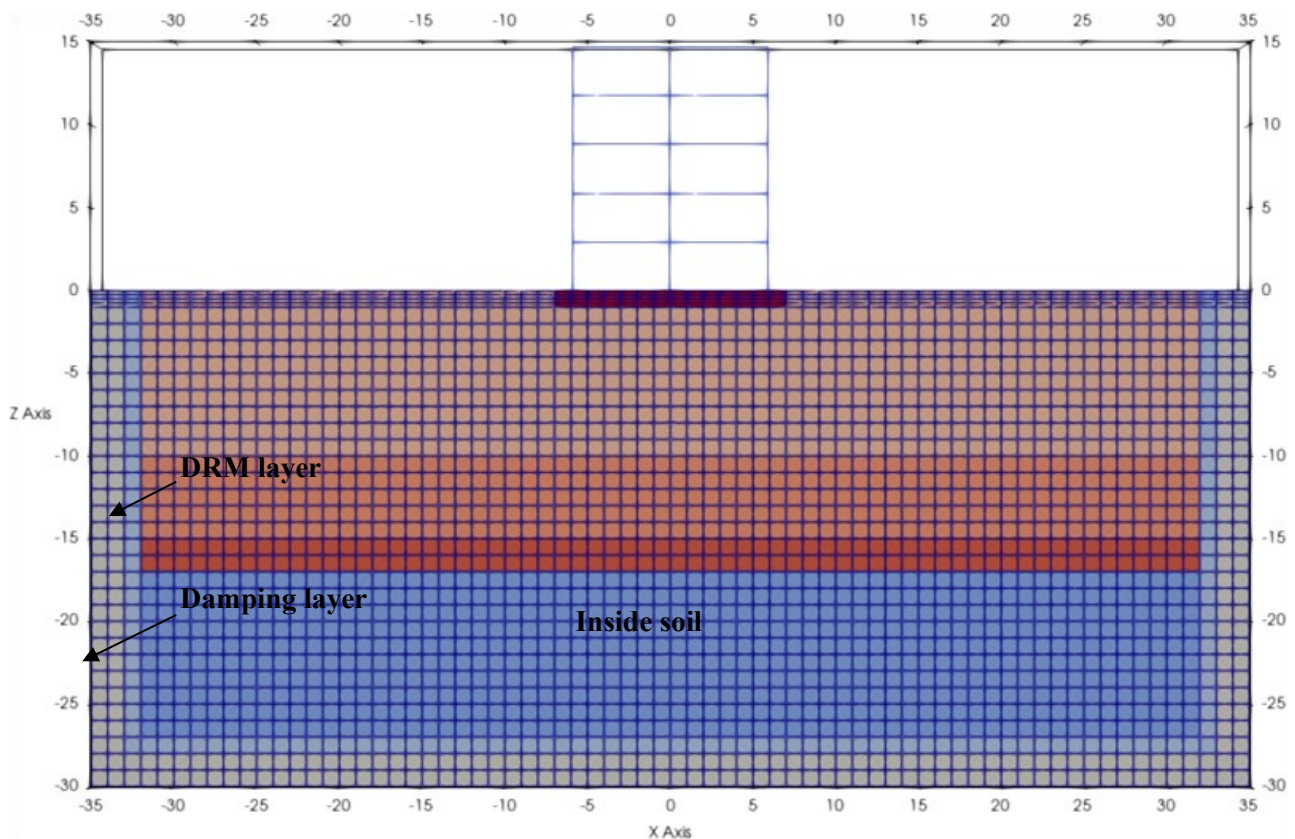


Figure 5. Numerical model of the analysed SPS system formed in Real-ESSI software

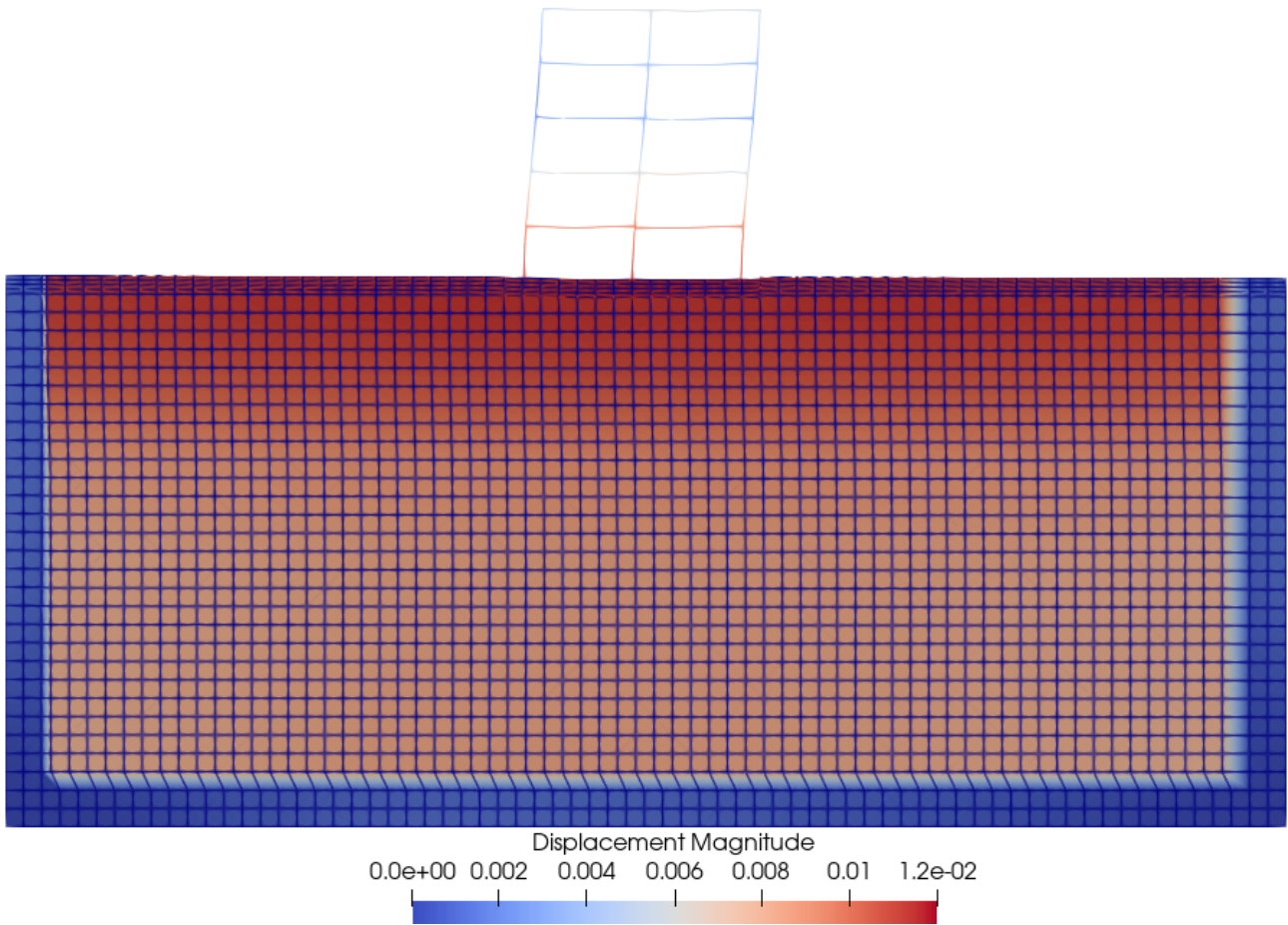


Figure 6. Deformed shape of analysed SPS system at the moment $t=5.37s$ of applied seismic excitation – $1 \times 1C$ DRM

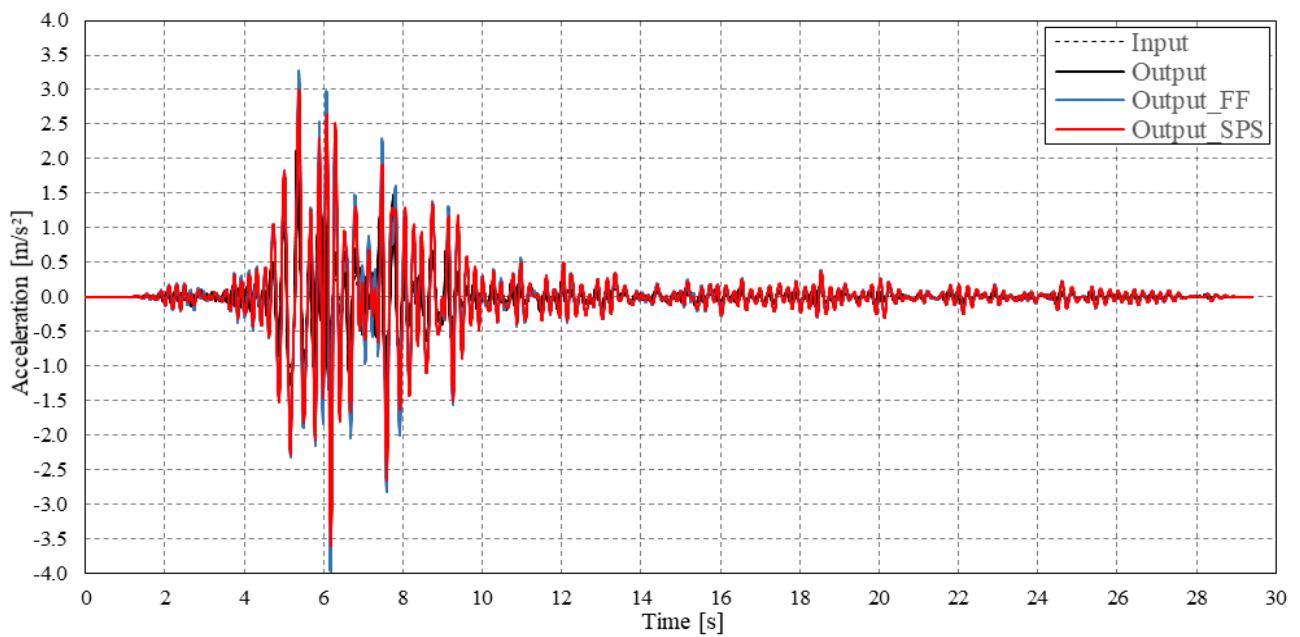


Figure 7. Horizontal acceleration recordings - complete time domain - $1 \times 1C$ DRM

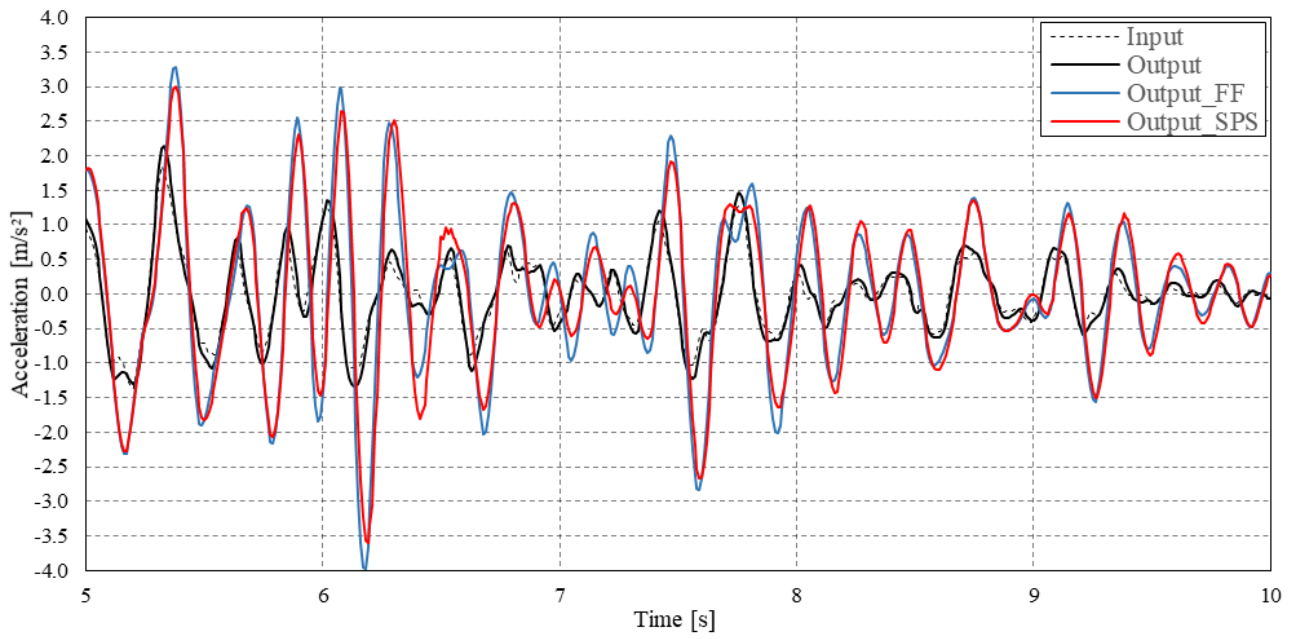


Figure 8. Horizontal acceleration recordings - interval between 5th and 10th second - $1 \times 1C$ DRM

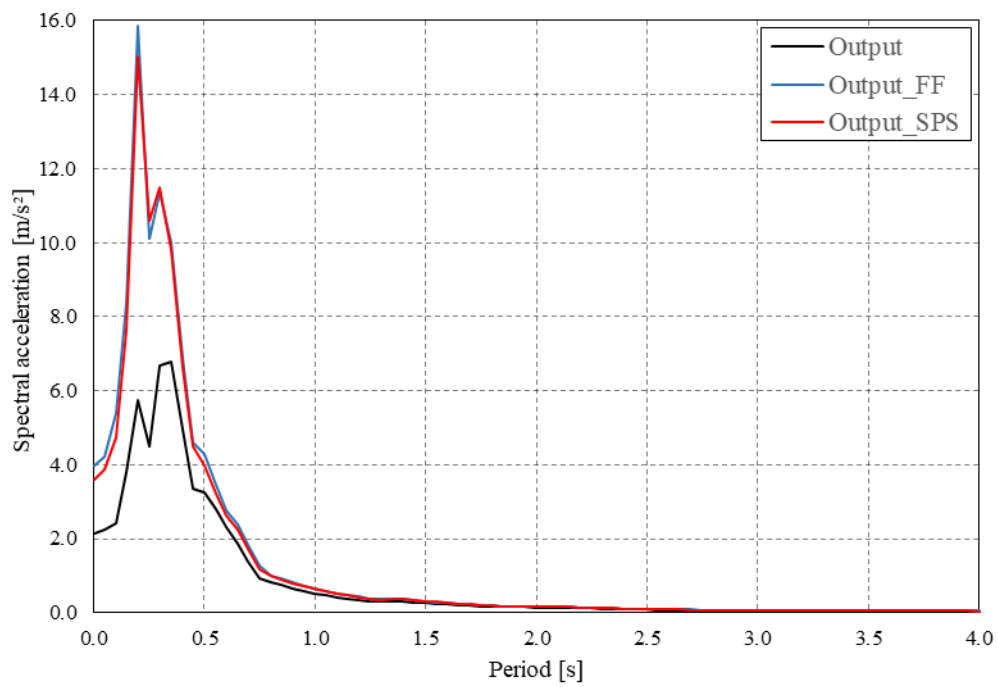


Figure 9. Horizontal acceleration elastic response spectra ($\xi=5\%$) - $1 \times 1C$ DRM

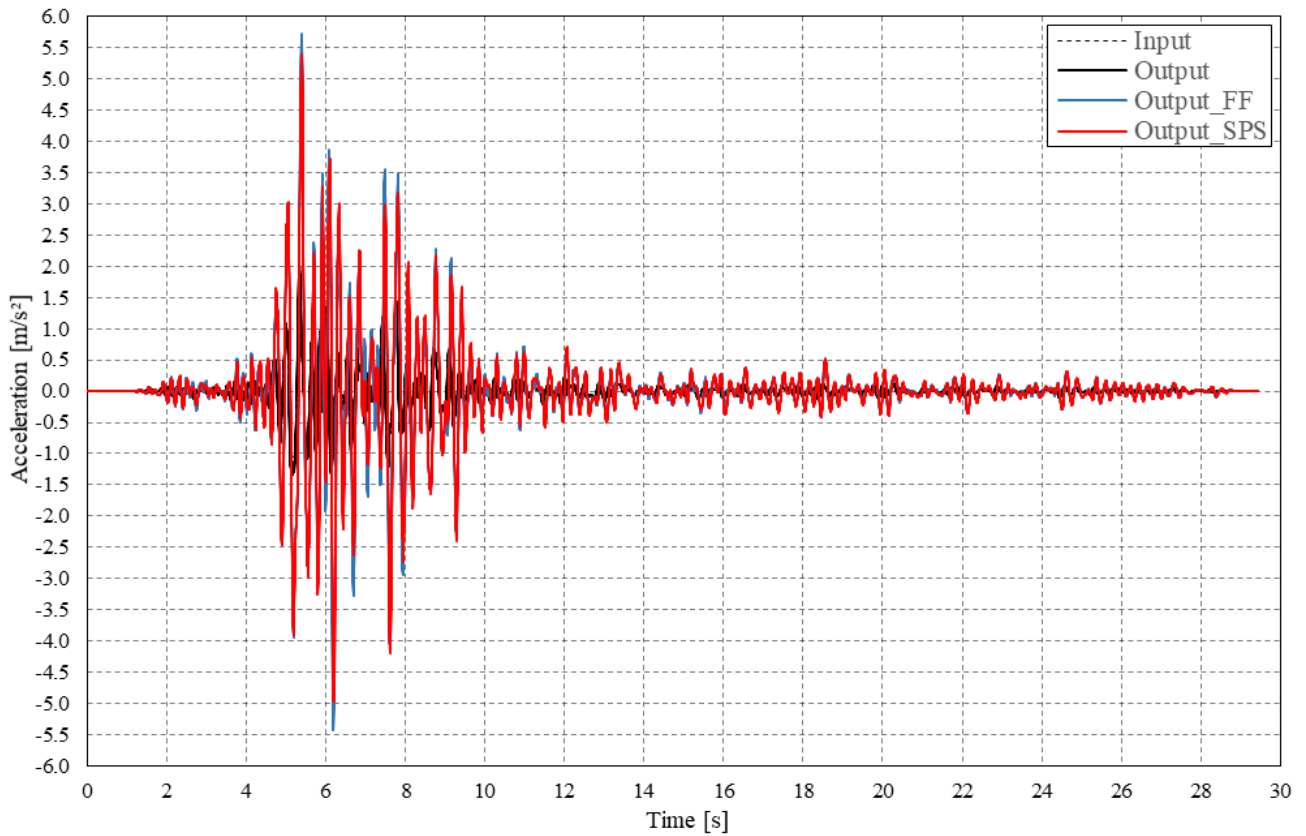


Figure 10. Horizontal acceleration recordings – complete time domain – 3C DRM

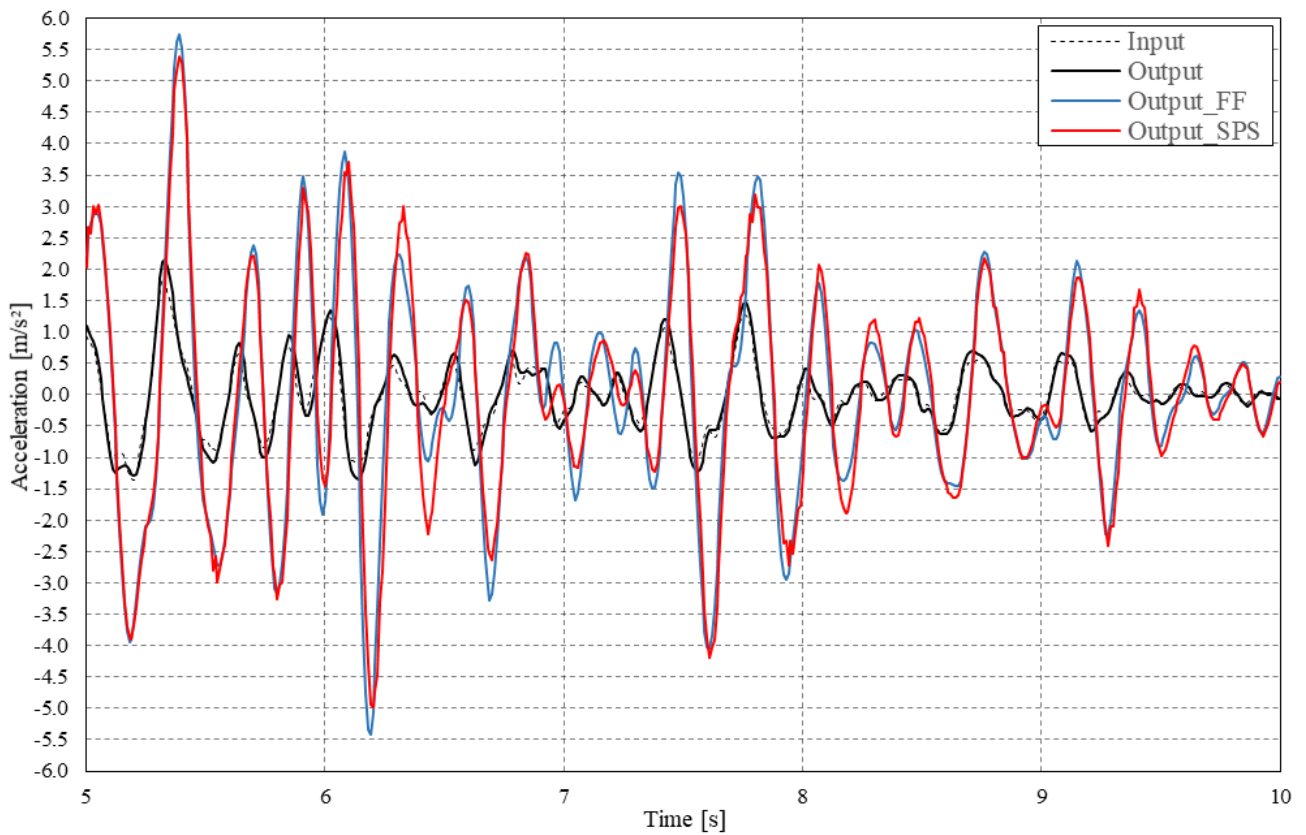


Figure 11. Horizontal acceleration recordings - interval between 5th and 10th second - 3C DRM

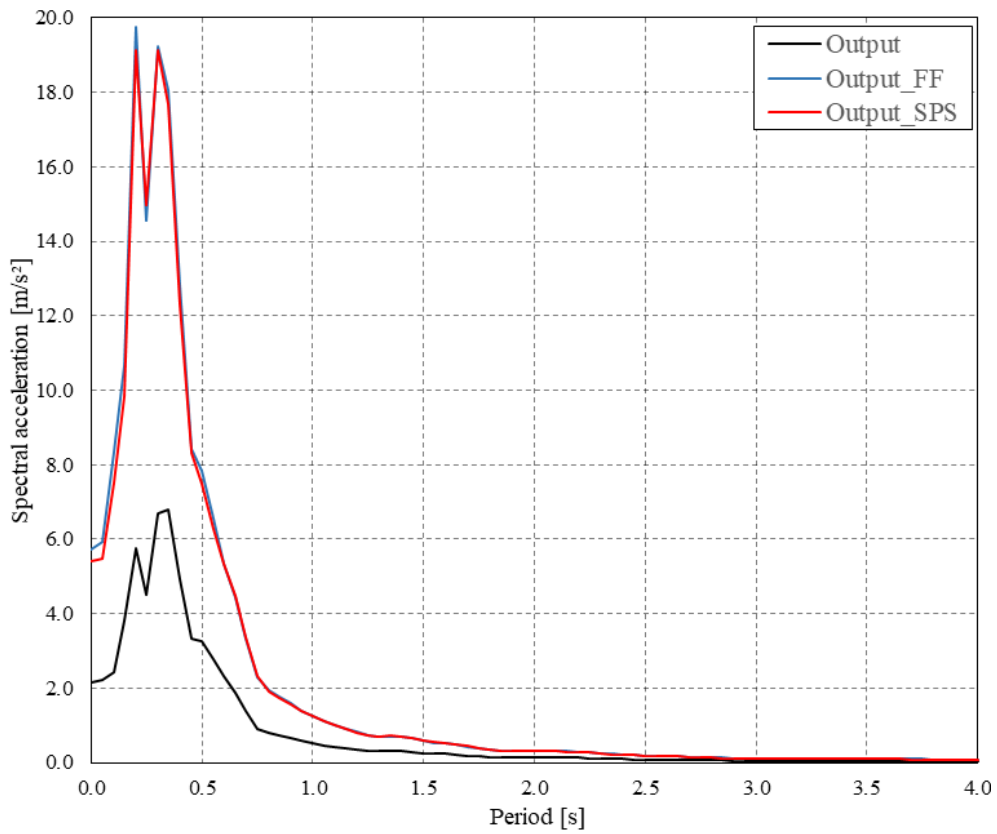


Figure 12. Horizontal acceleration elastic response spectra ($\xi=5\%$) – 3C DRM

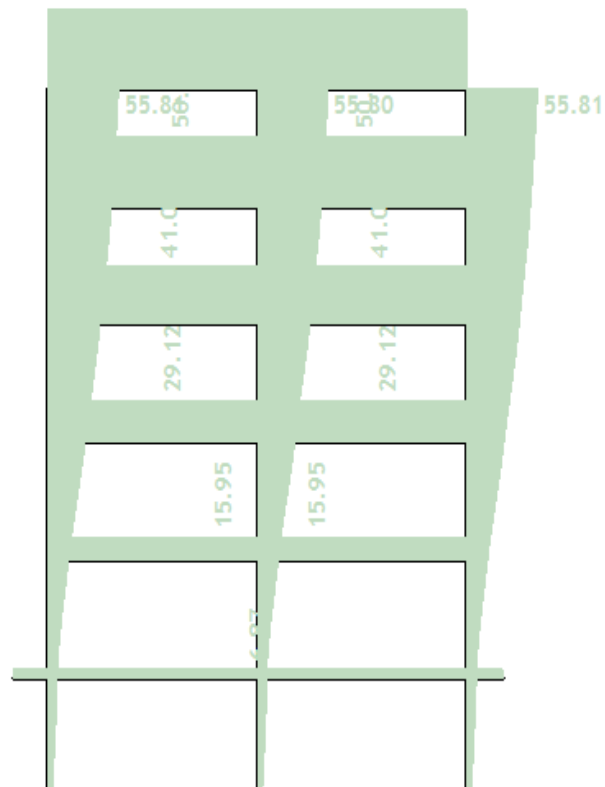


Figure 13. Horizontal displacement of RC pile-supported frame in mm – LE static seismic analysis – EC8 (Tower 6, Radimpex)

4.4 Discussion

Analyzing the presented results of the performed dynamic analyses, several interesting facts can be stated. Firstly, as a confirmation of the accuracy of the performed dynamic analyses, it can be stated that the horizontal acceleration recordings at the level of the bedrock "Input" and "Output" match practically perfectly. Secondly, it can be stated that very similar horizontal acceleration recordings "Output_FF" and "Output_SPS" are obtained for both types of DRM. The same applies to their response spectra. So, in this case, the piles follow the displacement of the surrounding soil during the earthquake and almost do not affect the seismic excitation of the superstructure (RC frame), regardless of the fact that piles are wedged in the bedrock at their lower end. Of course, the question is what would happen in cases with a larger number of piles of the same or larger diameter, which will be the subject of some future research. Thirdly, it is very important to note that in the case of the 3C DRM, a significantly higher maximum horizontal acceleration of the structure at the level of the pile cap beam was obtained compared to this acceleration in the case of the 1×1C DRM. This is quite obvious if the corresponding accelerograms, i.e., the corresponding horizontal acceleration elastic response spectra, are compared. Therefore, in the case of the 3C DRM, the superstructure is exposed to stronger lateral seismic forces. For this reason, the horizontal displacement of the top of the RC frame, which in the case of the 3C DRM is 7.38cm, is almost twice as large as the horizontal displacement of the top of the RC frame obtained in the case of the 1×1C DRM. Fourth, the area where the horizontal spectral acceleration is strongly amplified at the level of the pile cap beam compared to the level of the bedrock is much smaller in the 1×1C DRM than in the 3C DRM. This fact can be very important for the correct assessment of the lateral seismic load of structures. As expected, the zone of pronounced amplification of the horizontal spectral acceleration is located around the first (fundamental) natural time period of foundation soil, which is 0.237s. Finally, in LE static seismic analyses – EC8, horizontal displacement of the top of the RC frame is 5.58cm. It is significantly higher than in the case of the 1×1C DRM. However, it is significantly less (about 32%) than in the case of the 3C DRM. Greater horizontal displacement implies greater horizontal seismic forces.

5 Conclusion

The Domain Reduction Method (DRM) presented in this paper is significantly different from other methods used for seismic soil-structure interaction analysis. By applying the presented method, many aspects of this interaction, which are usually neglected in other methods for justified reasons, can now be analyzed. One of those aspects is the influence of surface seismic waves on the seismic response of the structure. In other words, it is about the influence of the different directions of propagation of body seismic waves through the soil profile from the source to the structure on its seismic response. This was demonstrated by performing linear-elastic, dynamic analyses of the seismic interaction of the foundation soil and the pile-supported structure using the DRM. It is about a specific type of seismic soil-structure interaction that cannot be analyzed in a sufficiently high-quality way using the usual seismic methods. Among other things, the obtained results point to the eventual possibility that the Lateral force seismic method, which is recommended by the Eurocode 8 standard for regular

structures and which is most often used in engineering practice, underestimates the level of the lateral seismic load of pile-supported structures. Of course, a firm conclusion can be drawn from the results of much more extensive and detailed research. This is a topic that the author will study in detail in the coming period.

Acknowledgements

The author would like to thank professor Jeremić from UC Davis (California), who made the REAL-ESSI simulation software available to the author and gave numerous advices on the use and theoretical basis of this software. The critical and helpful comments of reviewers are also highly appreciated.

References

- [1] J. Bielak, K. Loukakis, Y. Hisada, C. Yoshimura, Domain Reduction Method for Three-Dimensional Earthquake Modeling in Localized Regions, Part I: Theory, Bulletin of the Seismological Society of America 93 (2003) 817-824. <https://doi.org/10.1785/0120010251>
- [2] C. Yoshimura, J. Bielak, Y. Hisada, A. Fernandez, Domain Reduction Method for Three-dimensional Earthquake Modeling in Localized Regions, Part II: Verification and Applications, Bulletin of the Seismological Society of America 93 (2003) 825–840. <https://doi.org/10.1785/0120010252>
- [3] S. Kantoe, L. Zdravkovic, D. Potts, The domain reduction method for dynamic coupled consolidation problems in geotechnical engineering, International Journal for Numerical and Analytical Methods in Geomechanics 32 (2008) 659–680. <https://doi.org/10.1002/nag.641>
- [4] B. Jeremić, H. Yang, H. Wang, Seismic Ground Motions - On the Domain Reduction Method (DRM), Online Lectures: Realistic Modeling and Simulation of Earthquakes, and Soils, and Structures, and their Interaction (ESSI), Theory Background and Real-ESSI Examples Seismic Input, UC Davis, California, 2020. <http://sokocalo.engr.ucdavis.edu>
- [5] I. Herrera, J. Bielak, Soil–structure interaction as a diffraction problem, Proceedings of the 6th World Conference in Earthquake Engineering New Delhi 4 (1977) 19-24.
- [6] J. Bielak, P. Christiano, On the effective seismic input for nonlinear soil–structure interaction systems, Earthquake Engineering and Structural Dynamics 12 (1984) 107–119. <https://doi.org/10.1002/eqe.4290120108>
- [7] American Society of Civil Engineerings, Seismic Analysis of Safety-Related Nuclear Structures ASCE/SCI 4-16, 2016.
- [8] R. Borsutzky, T. Schubert, D. Kurmann, Application of the Domain Reduction Method in Seismic Analyses of Nuclear Power Plants, 26th International Conference on Structural Mechanics in Reactor Technology, Berlin, German, July 10-15 2022.
- [9] A. Pecker, B. Jeremic, J.J. Johnson, N. Orbovic, Methodologies for Seismic Soil-Structure Interaction Analysis in the Design and Assessment of Nuclear Installations, United Nations International Atomic Energy Agency UN-IAEA, (2022).

- [10] J.A. Abell, N. Orbović, D.B. McCallen, B. Jeremic, Earthquake soil-structure interaction of nuclear power plants, differences in response to 3-D, 3×1-D, and 1-D excitations. *Earthquake Engineering & Structural Dynamics* 47 (2018), 1478-1495.
<https://doi.org/10.1002/eqe.3026>
- [11] S. K. Sinha, Y. Feng, H. Yang, B. Jeremic, 3-D Non-Linear Modeling and Its Effects in Earthquake Soil-Structure Interaction, 24th International Conference on Structural Mechanics in Reactor Technology, Busan, Korea, August 20-25 2017.
- [12] B. Jeremic, N. Tafazzoli, T. Ancheta, N. Orbovic, A. Blahoianu, Seismic behavior of NPP structures subjected to realistic 3D, inclined seismic motions, in variable layered soil/rock, on surface or embedded foundations, *Nuclear Engineering and Design* 265 (2013) 85-94.
<https://doi.org/10.1016/j.nucengdes.2013.07.003>.
- [13] M.D. Trifunac, A note on rotational components of earthquake motions on ground surface for incident body waves, *Soil Dynamics and Earthquake Engineering* 1 (1982) 11-19.
- [14] V. Gičev, M.D. Trifunac, N. Orbović, Translation, torsion, and wave excitation of a building during soil-structure interaction excited by an earthquake SH pulse, *Soil Dynamics and Earthquake Engineering* 146 (2015) 391-401.
- [15] H. Wang, H. Yang, Y. Feng, B. Jeremić, Modeling and simulation of earthquake soil structure interaction excited by inclined seismic waves, *Soil Dynamics and Earthquake Engineering* 146 (2021) 106720
- [16] A.B. Vesic, Bending of Beams Resting on Isotropic Elastic Solid, *Journal of Soil Mechanics and Foundations Division ASCE* 87 (1961) 35 - 53.
<https://doi.org/10.1061/JMCEA3.0000212>